DMD Fast Forward. Published on September 28, 2011 as doi:10.1124/dmd.111.039503

DMD #39503

Cytoprotective effect of 20(S)-Rg3 on Benzo(α)pyrene-induced DNA damage

Po Ying Poon, Hoi Hin Kwok, Patrick Y. K. Yue, Mildred S. M. Yang, Nai Ki Mak,

Chris K. C. Wong, and *Ricky N. S. Wong

Department of Biology, Faculty of Science, Hong Kong Baptist University, Kowloon,

Hong Kong SAR, China

DMD Fast Forward. Published on September 28, 2011 as DOI: 10.1124/dmd.111.039503
This article has not been copyedited and formatted. The final version may differ from this version.

DMD #39503

Cytoprotective effect of 20(S)-Rg3 on BaP-induced DNA damage

*Corresponding author: Ricky Ngok Shun Wong

Address: Department of Biology, Faculty of Science, Hong Kong Baptist University, Kowloon, Hong Kong SAR, China

Telephone: (852)3411-7057

Fax: (852)3411-5995

Email: rnswong@hkbu.edu.hk

Number of text pages:36

Number of figures: 9

Number of references: 38

Number of words in the abstract: 247

Number of words in the introduction: 542

Number of words in the discussion: 1437

List of abbreviations:

BaP, Benzo(α)pyrene; HDFs, human dermal fibroblasts; HepG2 cells, Human hepatoma cells; NQO1, NAD(P)H: quinine oxidoreductase 1; Nrf2, nuclear factor

DMD Fast Forward. Published on September 28, 2011 as DOI: 10.1124/dmd.111.039503
This article has not been copyedited and formatted. The final version may differ from this version.

erythroid 2-related factor 2; PXR, pregnane X receptor; DMEM, Dulbecco's Modified Eagle Medium; FBS, fetal bovine serum; PBS, phosphate-buffered-saline; DMSO, dimethyl sulfoxide; DAPI, 4,6-diamidino-2-phenylindole dihydrochloride; MTT, 3-(4,5-dimethylthiazole-2-yl)-2,5-diphenyl-tetrazolium bromide; ROS, reactive oxygen species; RTKs, growth factor receptor tyrosine kinases; DMEs, Drug metabolizing enzymes; GST, glutathione S-transferase; UGT, uridine diphosphate glucuronyl transferase; SULT, sulfotransferases; SFN, L-sulforaphane

DMD Fast Forward. Published on September 28, 2011 as DOI: 10.1124/dmd.111.039503
This article has not been copyedited and formatted. The final version may differ from this version.

Abstract

Benzo(α)pyrene (BaP) is a polycyclic aromatic hydrocarbon ubiquitously existed in the environment. Its metabolites have been shown to cause DNA damage and cellular dysfunction in human. *Panax ginseng* C.A. Meyer is a Chinese medicinal herb, and ginsenosides are the main active constituent of ginseng. Accumulating evidences indicated that ginseng extract and ginsenosides possess cytoprotective effects. In this study, the protective effect of ginsenosides on BaP-induced DNA damage in human dermal fibroblasts (HDFs) and HepG2 cells was investigated. The genotoxic effect of BaP was measured by comet assay. Results showed that the tail moment was increased in BaP-treated cells, but co-treatment of ginsenoside 20(S)-Rg3 can significantly decrease BaP-induced DNA damage. Downstream mechanistic study revealed that 20(S)-Rg3 increased the gene expression of an important phase II detoxifying enzyme NAD(P)H: quinine oxidoreductase 1 (NQO1). The effect was also associated with the activation of protein kinase B (PKB/Akt) and nuclear translocation of nuclear factor erythroid 2-related factor 2 (Nrf2). These results indicated that 20(S)-Rg3 might protect HDFs from BaP-induced DNA damage through the activation of PI3K/Akt/Nrf2 pathway. Our results also demonstrated that 20(S)-Rg3 is a functional ligand of pregnane X receptor (PXR), a nuclear receptor

which mediates the induction of drug clearance pathways. Subsequent knockdown of PXR expression by small interfering RNA confirmed the involvement of PXR on the protective effects of 20(S)-Rg3 against BaP-induced DNA damage. In summary, ginsenoside 20(S)-Rg3 can protect BaP-induced genotoxicity in human cells, suggesting that ginseng may serve as a natural cytoprotective agent against environmental carcinogens.

DMD Fast Forward. Published on September 28, 2011 as DOI: 10.1124/dmd.111.039503
This article has not been copyedited and formatted. The final version may differ from this version.

Introduction

Benzo(α)pyrene (BaP) is a ubiquitous environmental contaminant found in smoke of incomplete combustion, diesel engine exhaust, fuel exhaust condensates, charbroiled food and cigarette smoke which is known to be mutagenic and carcinogenic. After absorption, BaP exerts its toxic effect through transformation by cytochrome P450 enzymes inside the cell to become reactive intermediates in causing DNA damage (Briedé *et al*., 2004). BaP metabolites can lead to different pathways of cytotoxicity, such as damage of macromolecules, impairment in cell functions and may finally cause carcinogenesis. Herbal substances and dietary phytochemicals are suggested as potential cytoprotective agents to maintain cellular functions (Jeong *et al*., 2004).

Ginseng is a Chinese traditional medicinal herb that has been used to promote longevity and immunity in China for thousands of years. Studies using different *in vitro* and *in vivo* models suggested that intake of ginseng may reduce the risk of several types of cancer (Nakata *et al*., 1998). Current research points out that the most important component of ginseng is ginsenosides because they account for most of the pharmacological effects (Attele *et al*., 1999). Ginsenosides are classified into three major categories by their chemical characteristics. They are: 20(S)-protopanaxadiol

(Rb1, Rg3, Rh2), 20(S)-protopanaxatriol (Re, Rf, Rg1) and oleanolic acid derivatives (de Smet, 2002).

The cytoprotective effect of ginsenosides has been demonstrated in various studies. Ginsenoside Rg3 exerts a cytoprotective effect towards DNA damage and cell apoptosis by reducing oxidative stress (Zang *et al*., 2008). Kwok *et al*. showed that ginsenoside 20(S)-protopanaxatriol protects endothelial cells against oxidative stress by regulating the intracellular redox status (Kwok *et al*, 2010). The underlying protective mechanisms may be due to the activation of intracellular survival signaling pathways. Akt is a central node that activates various downstream targets such as nuclear factor erythroid 2-related factor 2 (Nrf2) (Kim *et al*., 2010). Nrf2 is an important transcriptional factor of several detoxifying phase II enzymes, for example, NAD(P)H:quinine oxidoreductase 1 (NQO1) and heme oxygenase-1. Phase II enzymes, such as NQO1, can facilitate conjugation of BaP metabolites to increase their hydrophilicity so as to enhance their excretion from cells (Köhle and Bock, 2007).

On the other hand, pregnane X receptor (PXR), an orphan nuclear receptor, serves as a sensor of xenobiotics that mediates the induction of phase II enzymes and phase III transporters gene expression (Xu *et al*., 2005) for detoxification of potentially harmful substances. It was demonstrated that PXR protects HepG2 cells

from BaP-induced DNA damage. In PXR overexpressing liver cells, the mRNA levels of GSTM1, GSTA1, GSTA2, UGT1A6 and BCRP are upregulated upon the challenge of BaP (Naspinski *et al*., 2008). PXR can be activated by different herbal compounds such as *Ginkgo biloba* (Yeung *et al*., 2008) and St. John's wort (Moore *et al*., 2000). A study demonstrated that *Ginkgo biloba* extracts induce the expression of multiple drug metabolizing enzymes and transporters in cells through PXR (Li *et al*., 2009). Ginsenosides can also exert their effect through activation of nuclear receptors by acting as phytochemicals (Lee *et al*., 1997). Previous study illustrated that ginsenoside Rb1 can increase phase II enzymes through an estrogen receptor-related PI3K/Akt/Nrf2-dependent pathway (Hwang and Jeong, 2010).

In this study, we examined the cytoprotective mechanism of ginsenosides towards the BaP-induced DNA damage in human cells, and the possible involvement of PI3K/Akt/Nrf2 signaling and PXR pathway.

Materials and Methods

Chemicals and reagents

Dulbecco's Modified Eagle Medium (DMEM), fetal bovine serum (FBS), Opti-MEM, penicillin/streptomycin, phosphate-buffered-saline (PBS), and trypsin-EDTA were supplied by Gibco (Grand Island, USA). Benzo(α)pyrene (BaP), dimethyl sulfoxide (DMSO), 4,6-diamidino-2-phenylindole dihydrochloride (DAPI), 7-ethoxyresorufin, dicoumarol, LY294002, SR12813, propidium iodide, anti-actin and L-sulforaphane were purchased from Sigma (Saint Louis, USA). 3-(4,5-dimethylthiazole-2-yl)-2,5-diphenyl-tetrazolium bromide (MTT), agarose, Triton X-100 are purchased from USB (Cleveland, USA). Ginsenosides (purity>98%) were obtained from Fleton (Chengdu, China). Antibodies of PXR (N-16) were purchased from Santa Cruz (Santa Cruz, USA). PXR antibody was obtained from Novus Biologicals (Littleton, USA). Polyclonal antibodies, such as anti-Akt, phospho-Akt (Ser473), Erk and phospho-Erk (Thr202/Tyr204) were obtained from Cell Signaling (Beverly, USA).

Cell culture and treatment

Neonatal human dermal fibroblasts (HDFs) were obtained from Lonza

(Walkersville, USA) and Human hepatoma cells (HepG2 cells) were purchased from American Type Culture Collection (Rockville, USA). The cells were cultured in 100 mm^2 tissue culture dish with DMEM supplemented with 10 % FBS and 1 % penicillin/streptomycin. Cells were maintained in a humidified incubator with 5 % CO_2 at 37 °C.

Cells were starved with serum-free DMEM overnight before drug treatment. Cells were then treated with BaP in the presence or absence of ginsenosides in DMEM (DMSO ≤ 0.1%).

MTT proliferation assay

HDFs were seeded at a density of 2 x 10^4 cells per well in 96-well plate overnight. After drug treatment for 24 h, MTT (20 µl) was added to each well and incubated for 3 h. Then, the medium were discarded and 100 µl DMSO was added to dissolve the formazan salts in each well. The optical density (O.D.) was measured with the microplate spectrophotometer (Infinite F200, Tecan, Switzerland) at 540 and 690 nm. Cell viability was calculated according to the equation: ($OD_{sample} - OD_{blank}$ / $OD_{control} - OD_{blank}$) x 100%.

Alkaline single cell gel electrophoresis assay (Comet assay)

HDFs and HepG2 cells were plated in 6-well plates at a density of 2 x 10^5 cells per well. After drug treatment for 24 h, cells were harvested by trypsinization, then cell suspensions were mixed with agarose (0.65%) and the mixture was pour onto an agarose pre-coated semi-frosted microscopic slide followed by covering the agarose gel with coverslips. The coverslips were removed gently after the agarose gel was set at room temperature. The cells were lysed in ice-cold lysis solution (pH 10.0) at 4 ºC for 1 h and then incubated in electrophoresis buffer (pH 13.5) for 30 min, and subsequently subjected to electrophoresis at a constant current of 250 mA for 6 min. The slides were then rinsed in neutralizing buffer (pH 7.5) and immersed in water at 4 ºC until observation. The DNA was stained with propidium iodide (10 μg/ml) for 30 min. The comet image was captured by invert microscope (Carl Zeiss) equipped with cool-CCD camera (Apogee). Tail moment of 200 comets of each individual treatment group was analyzed using CometScore v1.5 (TriTek, Sumerduck, USA) and at least three independent experiments were performed.

Terminal dUTP nick end labeling (TUNEL)

TUNEL assay was performed using the *In Situ* Cell Death Detection Kit (Roche Diagnostics, Mannheim, Germany) according to the manufacturer's instructions. Briefly, after drug treatment, HDFs were fixed with 4 % paraformaldehyde in PBS at

room temperature for 1 h. After fixation, cells were washed with PBS and were permeabilized by 4 % ice-cold paraformaldehyde. Cells were then incubated with TUNEL reaction mixture for 1 h at 37 ºC. The labelled cells were assayed using flow cytometer (Becton Dickinson FACSorter, Rutherford, NJ) with excitation at 488 nm and emission at FL-1 channel. The percentage of TUNEL-positive cells was analyzed by CELLQuest software (Becton Dickinson, San Jose, USA).

Western Blotting

After drug treatment, HDFs were lysed with CytoBuster protein extraction reagent (Novagen, Madison, USA) containing Protease Inhibitor Cocktail Set III (1:200 v/v) (Calbiochem, La Jolla, USA). The cell lysate was centrifuged at 20,800 g for 15 min at 4 °C. After centrifugation, supernatant was collected and protein content was determined by Dc protein assay (Bio-Rad, Hercules, USA). Equal amounts of protein were separated by 10 % SDS-PAGE and transferred to nitrocellulose membrane (GE Healthcare, Piscataway, USA). The membrane was subsequently blocked with non-fat milk in TBS-T for 1 h at room temperature, and followed by probing with diluted primary antibodies for 3 h at room temperature. The membrane was further incubated with secondary antibodies for 1 h at room temperature. Finally, protein bands were revealed by exposure to medical X-ray film after incubation with chemiluminescence

substrate (Bio-Rad).

Immunofluorescence staining

HDFs were seeded at a density of 1 x 10^4 cells on a coverslip in a 24-well plate overnight. The cells were fixed with 4 % paraformaldehyde for 15 min at room temperature. The fixed cells were then permeabilized with Triton X-100 (0.2 %) in PBS for 15 min. The cells were incubated with primary antibody (1:200 dilution) overnight at 4 °C. After washing with PBS, the cells were incubated with secondary antibodies (PE antibody 1: 250 dilution) for 2-3 h in dark at room temperature. Nucleus were visualized with DAPI (0.5 μg/ml) staining. The washed coverslip was mounted on the slides using DAKO fluorescence mounting medium (Vector Laboratories, Burlingame, USA) in dark, and images were captured using an Olympus FV1000 confocal scanning laser microscope (Olympus, Essex, UK).

Real time reverse transcriptase polymerase chain reaction

Total RNAs were extracted with TRIzol reagent (Invitrogen, Carlsbad, USA) and reverse transcribed using Superscript III First-strand Synthesis SuperMix (Invitrogen). Amplification of cDNA with custom oligonucleotides as primers was carried out with PCR SuperMix (Bio-Rad). Real-time PCR was performed in the following thermal

profile: 95 °C, 10 min, 1 cycle; 95 °C, 30 seconds, 55 °C, 1 min, 72 °C, 1 min, 40 cycles. The primers were as follows: GAPDH-forward primer: 5'-ATCAGCAATGCCTCCTGCAC-3', reverse primer 5'-TGGTCATGAGTC -CTTCACG-3', NQO1 forward primer 5'- CAAATCCTGGAAGGATGGAA-3', reverse primer: 5'-GGTTGTCAGTTGGGATGGAC-3' (Invitrogen). Real-time PCR reactions were conducted using iCycler iQ real-time PCR detection System (Bio-Rad). The data were then normalized using the expression levels of GAPDH mRNA.

PXR Competitive Binding Assay

Binding affinity of ginsenosides with PXR was determined by the LanthaScreen PXR (SXR) Competitive Binding Assay (Invitrogen) according to the manufacturer's instructions. Serial dilutions of SR-12813 (0.03 nM to 100 μM), 20(S)-Rg3 and 20(R)-Rg3 (0.01 μM to 50 μM) were used to compete with a fluorescent PXR ligand for binding to human PXR. The fluorescence resonance energy transfer (FRET) signal was then measured by a spectrophotometer (Infinite F200, Tecan, Switzerland). The binding curves were fitted with a two-state one-site competition model by the Prism software (GraphPad software, Inc., San Diego, USA).

Small interfering RNA (siRNA) transfection assay

DMD Fast Forward. Published on September 28, 2011 as DOI: 10.1124/dmd.111.039503
This article has not been copyedited and formatted. The final version may differ from this version.

Three pairs of siRNA targeting human PXR (Ambion, Austin, USA) were used, HepG2 cells were seeded into 24-well plates at a density of 7.5×10^4 cells per well overnight before transfection, then siRNA (20 nM) and siLentFect transfection reagent (1 ul) (Bio-Rad) were mixed in 50 μl Opti-MEM and incubated for 15 mins prior to transfection. Non-Targeting siRNA (20 nM) (Thermo Scientific Dharmacon, Lafayette, USA) was used in parallel with the si-PXR. Drug treatment was performed 24 h after transfection." The sequences of si-PXR are listed below, sense: 5'-GUCCUACAUUGAAUGCAAUtt-3', antisense 5'-AUUGCAUUC- AAUGUAG -GACtt-3', sense 5'-GACACUACCUUCUCCCAUUtt-3', antisense 5'-AAUGGG -AGAAGGUAGUGUCaa-3', sense 5'-GGCUAUCACUUCAAUGUCAtt-3', antisense 5'-UGACAUUGAAGUGAUAGCCag-3'

Statistical analysis

Each experiment was repeated at least three times. Data were expressed as mean ± S.D. Statistical analyses were carried out by comparing different data sets using Student's *t* test.

Results

Genotoxicity of benzo(α)pyrene

The effect of BaP on DNA damage and viability of HDFs was determined by comet assay and MTT viability assay, respectively. After 24 h treatment, BaP (0.1 – 50 μM) was found to induce DNA damage and cell death in a dose-dependent manner (Fig. 1). BaP, at the concentrations of >10 μM, induced significant DNA damage (Fig. 1A, B) and cell death in HDFs (Fig. 1C) when compared with control.

Protective effects of ginsenosides on BaP-induced DNA damage in HDFs

Ginsenosides have previously been shown to possess cytoprotective effect (Kwok *et al*., 2010). Therefore, the protective effect of ginsenosides (Rg1, Rb1, 20(S)-Rg3 and 20(R)-Rg3) (Supplemental Figure 1) on BaP-induced HDFs DNA damage was investigated. As shown in Fig. 2A, treatment of HDFs with BaP (10 μM) resulted in about 30 % cell death. In the presence of 20(S)-Rg3 (10 μM), cytotoxic effect of BaP was totally abolished. However, other ginsenosides, such as Rg1, Rb1, or 20(R)-Rg3 showed no significant protection towards BaP-induced cell death. The cell viability of HDFs treated with 20(S)-Rg3, 20(R)-Rg3, Rg1 and Rb1 alone are about 124%, 105%, 98% and 91%, respectively (Supplemental Figure 2).

DMD Fast Forward. Published on September 28, 2011 as DOI: 10.1124/dmd.111.039503
This article has not been copyedited and formatted. The final version may differ from this version.

BaP-induced DNA strand breakage was then determined by TUNEL assay. The percentage of TUNEL-positive cells in the control and BaP treatment group was 2.39 % and 15.96 %, respectively. Among the different ginsenosides: 20(S)-Rg3, 20(R)-Rg3, Rg1 and Rb1, 20(S)-Rg3 was the most effective in reducing BaP-induced DNA strand breakage from 15.96 % (BaP-treatment group) to 3.07 % (Fig. 2B). 20(R)-Rg3 and Rb1 was found to decrease TUNEL-positive cells to 12.76 % and 9.77 %, respectively, while Rg1 cannot exert similar protection on DNA strand breakage (Fig. 2B). The cytoprotective effect was further confirmed by the comet assay. BaP alone increased the mean tail moment while in the presence of 20(S)-Rg3, tail moment was significantly reduced in the HDFs; whereas other ginsenosides did not show similar cytoprotective effect (Fig. 2C).

Role of PI3K in 20(S)-Rg3-mediated cytoprotection

PI3K/Akt signaling pathway has a major role in regulating cell survival. LY294002, a specific inhibitor of PI3K (IC_{50} ~ 0.31uM for PI3Kβ), LY294002 is widely used in studying the involvement of PI3K/Akt mechanism. Therefore it was used to determine the role of PI3K in the protective mechanism of 20(S)-Rg3 in HDFs. From the result of comet assay, the mean tail moment of BaP alone was 16 ± 1.5, and it was reduced to 0.3 ± 0.3 after co-treatment with BaP and 20(S)-Rg3 (Fig. 3).

DMD Fast Forward. Published on September 28, 2011 as DOI: 10.1124/dmd.111.039503
This article has not been copyedited and formatted. The final version may differ from this version.

However, pretreatment of HDFs with LY294002 before BaP and 20(S)-Rg3 co-treatment resulted in the mean tail moment of 14.7 ± 1.4, and the value was very similar to BaP treated HDFs (16 ± 1.5). This observation suggested that the PI3K/Akt pathway might be involved in the cytoprotective effect of 20(S)-Rg3.

Effect of benzo(α)pyrene and 20(S)-Rg3 on the activation of Akt and Erk

Results from Western blotting analysis indicated that 20(S)-Rg3 induced phosphorylation of both Akt (Ser473) and Erk (Thr202/Try204). BaP alone exerted no effect on the phosphorylation activation of Akt and Erk. 20(S)-Rg3 was able to activate Akt and Erk in a time-dependent manner, and the peak of phosphorylation of Akt and Erk was at around 30 min (Fig. 4).

Role of PI3K/Akt pathway in Nrf2 activation

Nrf2 is an important transcriptional factor that induces the expression of phase II enzymes. Thus, the effects of 20(S)-Rg3 and BaP on the nuclear translocation of Nrf2 were examined. Cells treated with 20(S)-Rg3 alone or co-treatment with BaP and 20(S)-Rg3 showed a significant increase in Nrf2 staining in the nucleus (Fig. 5). Less immunoreactivity of Nrf2 staining was observed in the nucleus of control cells treated with BaP-alone or DMSO. This result clearly indicated that 20(S)-Rg3 could

DMD Fast Forward. Published on September 28, 2011 as DOI: 10.1124/dmd.111.039503
This article has not been copyedited and formatted. The final version may differ from this version.

induce the nuclear translocation of Nrf2. To further address the role of PI3K/Akt pathway in 20(S)-Rg3-induced Nrf2 translocation, LY294002 was used to block the PI3K→Akt pathway. After pretreatment with LY294002 (10 μM) for 1 h, 20(S)-Rg3-induced Nrf2 translocation was abolished (Fig. 5). This observation indicates that 20(S)-Rg3-induced Nrf2 translocation is PI3K/Akt dependent. SFN, a phase II enzyme inducer which has been shown to disrupt Nrf2-Keap1 complex and allows the free translocation of Nrf2 into the nucleus, was used as a positive control to demonstrate the nuclear translocation of Nrf2.

Effect of 20(S)-Rg3 on NQO1 mRNA expression

NQO1, an important phase II enzyme responsible for conjugation of metabolites to enhance BaP elimination, is one of the transcriptional targets of Nrf2. It was revealed that co-treatment of 20(S)-Rg3 (10 μM) with BaP in HDFs could increase NQO1 gene expression in about 2-fold when compared with BaP alone (Fig. 6). Hence, NQO1 expression is possibly induced by Nrf2 translocation upon 20(S)-Rg3 treatment, and may subsequently enhance the export of BaP metabolites.

TR-FRET competitive binding assay of PXR with Rg3 and SR-12813

Previous studies indicated that ginsenosides may bind on different nuclear

receptor such as glucocorticoid receptor or estrogen receptor, to exert diverse physiological responses; however, little is known about the effect of ginsenosides on PXR. PXR, a sensor of xenobiotics involved in drug clearance pathways, can be activated by a wide spectrum of steroids and pharmaceutical agents. As PXR is barely expressed in HDFs (Supplemental Figure 3) (Chang *et al.*, 2008; Naspinski *et al.*, 2008), we use human hepatoma HepG2, which express high level of PXR, as cellular model to study the possible involvement of PXR in 20(S)-Rg3-induced protection against BaP. Here we examine the effects of 20(S)-Rg3 on PXR. First, to test the specific binding affinity of Rg3 to PXR, PXR competitive ligand binding assay was performed (Fig. 7). The binding affinity of 20(S)-Rg3 was found to be comparable with the potent synthetic PXR ligand SR12813. The data suggested that 20(S)-Rg3 is a high-affinity PXR agonist.

Role of PXR in 20(S)-Rg3-mediated protection

The involvement of PXR in the cytoprotective effect of 20(S)-Rg3 against BaP-induced DNA damage was confirmed by decreasing the expression of PXR using siRNA. Depletion of PXR by specific siRNA in HepG2 cells was verified by Western blot analysis (Fig. 8A). Similar to HDFs, DNA damage induced by BaP (10 μM) can also be reduced by 20(S)-Rg3 in HepG2 cells (Fig. 8B). However, knockdown of

DMD Fast Forward. Published on September 28, 2011 as DOI: 10.1124/dmd.111.039503
This article has not been copyedited and formatted. The final version may differ from this version.

PXR abolished the protective effect of 20(S)-Rg3 against BaP-induced DNA damage. This observation suggested that PXR is also involved in the protective mechanism of 20(S)-Rg3.

Discussion

BaP, a typical environmental pollutant present mainly in cigarette smoke, barbecued meat and smoked food, has been implicated to increase the risk of cancer. Human is constantly exposed to BaP through skin and gastrointestinal absorption. Skin is the largest organ of the human body which protects the body from chemicals, fungal, bacterial and viral pathogens. Dermis is the structural layer of skin, but it is also one of the sites for drug metabolism, as skin cell expresses drug-metabolizing enzymes (DMEs) which are essential for metabolism and removal of xenobiotics. In case of direct contact (i.e. skin painting), or lesion of skin, xenobiotics can penetrate into the skin and down to the dermis layer where fibroblast is found. On the other hand, liver plays a central role in detoxification of endobiotics and xenobiotics in human body. Ingested xenobiotic in food is absorbed by digestive tract and then delivered to the liver through the portal blood (Malhi *et al*., 2010). Liver cells express high level of DMEs which can facilitate the elimination of the xenobiotics, such as BaP, from the body, thus protect the body from toxicity. Failure in removal and accumulation of xenobiotics may result in genetic damage and finally leading to cell mutagenicity and cancer induction.

In human cells, BaP undergoes sequential metabolic reactions catalyzed by cytochrome P450s (i.e. CYP1A1), and epoixde hydrolase to produce primary reactive

metabolites (epoxides and hydroxy metabolites) which further metabolized to diols, diol epoxides and quinones. Diol epoxide (i.e. BP-7,8-diol-9,10-epoxide) is an ultimate reactive metabolite which can generate DNA adducts and DNA breakages. Furthermore, reactive oxygen species (ROS) may be produced during the autooxidation of 6-OH BaP to quinones, superoxide, hydroxyl radicals and hydrogen peroxide produced through redox-cycle can lead to oxidative DNA adducts (Miller and Kenneth, 2001) and disrupt cellular redox balance.

From the results, BaP significantly induced DNA damage (Fig. 1A, B) and cell death (Fig. 1C). DNA damage caused by BaP may due to the formation of ultimate carcinogenic metabolites metabolized by phase I enzyme. BPDE is one of the major final metabolites which can cause damage to DNA and disrupts cell functions.

Ginseng is a traditional Chinese medicine. The most important pharmacological components in ginseng are ginsenosides which have various bioactivities as revealed in many systems, such as, antioxidation (Kwok *et al*., 2010) and cytoprotection (Chan *et al*., 2004). In the present study, we demonstrated cytoprotective effect of ginsenosides. Among the 30 types of well known ginsenosides, Rb1 is the most abundant ginsenoside under 20(S)-protopanaxadiol category in American ginseng (*Panax quinquefolius*) and Rg1 is one of the most abundant ginsenosides among the 20(S)-protopanaxatriol category in Chinese ginseng (*Panax ginseng*) (Court, 1996).

Besides, Rg3 is one of the major ginsenosides found in red ginseng (Wang *et al*., 2007). Ginsenoside Rg3 exists as stereoisomer pair, 20(S)-Rg3 and 20(R)-Rg3, which differs in the position of hydroxyl group on the chiral center at carbon-20. Park and co-workers showed that 20(S)-Rg3 and 20(R)-Rg3 exhibited differential pharmacological effects (Park *et al*., 2008).

20(S)-Rg3 was found to be the most effective ginsenoside to protect cells against the challenge of BaP in our present study. 20(S)-Rg3 showed protection on cell death (Fig. 2A) and DNA damage (Fig. 2B, C) after treatment with BaP. Many evidences have already showed that 20(S)-Rg3 has anti-carcinogenic (Yun *et al*., 2001) and anti-apoptotic activity (Min *et al*., 2006). Our present results indicated that only 20(S)-Rg3 can possess major cytoprotective effect towards DNA damage and cell death. PI3K/Akt is regarded as a cell survival regulator which regulates diverse physiological responses including proliferation and cell survival (Yong and Mien-Chie, 2010). PI3K can be activated by growth factor receptor tyrosine kinases (RTKs) or G protein-coupled receptors (Liao *et al*, 2010). Our previous finding also demonstrated that ginsenosides can activate PI3K/Akt pathway (Sengupta *et al*., 2004). In the present study, 20(S)-Rg3 can rapidly activate the phosphorylation of Akt (Fig. 4) and protect cells from BaP-induced DNA damage and cell death. Ginsenoside Rg1 has been shown to activate mitogen-activated protein kinases and Akt through

interacting with IGF-1 and FGF-2 signaling (Lu *et al*, 2009). Thus, 20(S)-Rg3 may activate PI3K/Akt in a RTKs dependent manner. Activated Akt can lead to different cellular signaling, such as promoting cell survival by inhibition of phosphorylation of pro-apoptotic protein Bad (Manning and Cantley, 2007), which can prevent BaP-induced cell death in HDFs.

Nrf2 is a master transcriptional factor of phase II detoxifying and antioxidant enzymes (Hsieh *et al*., 2009). It has been shown that activation of Akt can induce phosphorylation of Nrf2 and leads to nuclear translocation from cytoplasm (Wang *et al*., 2008). The translocated Nrf2 can promote phase II detoxifying and antioxidant enzymes gene transcription to facilitate the xenobiotics elimination process. It is believed that a series of DME would be modulated in our system as well. By using LY294002, inhibitor of PI3K, we showed that 20(S)-Rg3-induced Nrf2 translocation can be abolished indicating the involvement of the PI3K/Akt.

Drug metabolizing enzymes (DMEs) take part in the metabolism and elimination of xenobiotics (Meyer, 1996). DMEs include phase I, phase II metabolizing enzymes and phase III transporters. Gene expression of phase II enzymes, such as glutathione S-transferase (GST) P1, uridine diphosphate glucuronyl transferase (UGT) 1A1, sulfotransferases (SULT) 1A1 and NQO1, can be induced by Nrf2. They may enhance the hydrophilicity and excretability of the BaP metabolites (Köhle and Bock, 2007).

Therefore, we further investigated the involvement of DMEs in 20(S)-Rg3 mediated detoxification. In our study, we demonstrated the increase of NQO1 gene expression in HDFs after treatment with 20(S)-Rg3, this indicated that the detoxification action of 20(S)-Rg3 may be associated with NQO1 induction. NQO1 detoxifies quinones to quinols (Ross, 2004), then quinols can be further conjugated by UGTs and SULTs, and subsequently excreted through multidrug resistance-associated proteins (Xu *et al*, 2005). Even thought, we have not demonstrated the involvement of UGTs and SULTs; however, we predicted that the detoxifying action of 20(S)-Rg3 would enhance further conjugation.

Recent studies demonstrated that PXR can directly regulate phase II enzymes and phase III transporters gene expressions (Nakata *et al*., 2006). Pregnane X receptor (PXR; NR1I2), also known as steroid and xenobiotic receptor (SXR) or pregnane activated receptor (PAR), is an orphan nuclear receptor. It is an important component of the body's adaptive defense mechanism against toxic substances. It serves as a sensor of xenobiotics that mediates induction of drug clearance pathways to ensure rapid detoxification of potentially harmful substances. It has been demonstrated that ginsenosides can act as phytochemicals to exert their effect through activation of nuclear receptors (Lee *et al*., 1997). Interestingly, binding study showed that 20(S)-Rg3 but not 20(R)-Rg3 can act as functional ligand of PXR (Fig. 7). Activated

PXR can regulate the expression of metabolic enzymes and transporters in order to protect cells from toxic xenobiotics (Naspinski *et al*., 2008). As mentioned previously, 20(S)-Rg3 and 20(R)-Rg3 are stereoisomers that differ in the position of hydroxyl group carbon-20. This study pointed out that stereoisomer of natural compound is critical in their pharmacological action. Upon PXR binding, gene expression of DME in different phases may be induced. In order to validate the role of PXR in the proposed mechanism, we employed human hepatic cells expressing human PXR as a study model. By means of RNA interference, the intrinsic PXR was artificially depleted and the results indicated that the protective effect of 20(S)-Rg3 is critically related to PXR. This finding is in agreement with many literatures that PXR is involved in inducing different DMEs for cytoprotection. For example, activation of PXR by *Ginkgo biloba* terpenoids induces the expression of multiple hepatic DMEs and transporters, and thus may protect against the toxicity of PAHs, such as BaP (Li *et al*., 2009).

Pharmacokinetic study on human subjects using HPLC-MS demonstrated that after intake of 20(S)-Rg3 (60 mg), the plasma concentration of 20(S)-Rg3 ranged from 2.5 to 1000 ng/ml (0.003 μM to 1.278 μM) (Wang *et al*., 1999; Zhao *et al*., 2010), which is relatively lower than the concentration used in the present study (10 μM). However, as an herbal tonic with low toxicity, ginseng or ginsenosides are

consumed regularly to improve vitality in Eastern countries. As a result, the concentration of 20(S)-Rg3 in plasma may gradually increase to a level close to the present study. However, further *in vivo* studies are required to elucidate the beneficial effects of ginseng against toxic effect of environment contaminants.

In conclusion, 20(S)-Rg3, one of prevalent effective components of ginseng, was shown to inhibit BaP-induced DNA damage through PI3K/Akt/Nrf2 and PXR pathways (Fig. 9). The result uncovered a potential protective effect of ginsenoside against exposure to environmental contaminants, this warrants further study on the cytoprotective effect of ginsenoside under long-term consumption.

Authorship Contributions

Participated in experimental design: Poon, Kwok, Yue

Conducted experiments and data analysis: Poon

Provide BaP: CKC Wong

Project design: Yang, RNS Wong

Manuscript preparation: Poon, Kwok, Yue, RNS Wong, Mak

References

Akintobi AM, Villano CM and White LA (2007) 2,3,7,8-Tetrachlorodibenzo-p- dioxin (TCDD) exposure of normal human dermal fibroblasts results in AhR-dependent and -independent changes in gene expression. *Toxicol Appl Pharmacol* **220**: 9-17.

Attele AS, Wu JA and Yuan CS (1999) Ginseng pharmacology: multiple constituents and multiple actions. *Biochem Pharmacol* **58**: 1685-1693.

Briedé JJ, Godschalk RW, Emans MT, De Kok TM, Van Agen E, Van Maanen J, Van Schooten FJ and Kleinjans JC (2004) *In vitro* and *In vivo* studies on oxygen free radical and DNA adduct formation in rat lung and liver during benzo(α)pyrene metabolism. *Free Radic Res* **38**: 995-1002.

Chan K, Chui SH, Wong DY, Ha WY, Chan CL and Wong RN (2004) Protective effects of Danshensu from the aqueous extract of *Salvia miltiorrhiza* (Danshen) against homocystein-induced endothelial dysfunction. *Life Sci* **75**: 3157-3171.

Chang KCN, Shen Q, Oh IG, Jelinshky SA, Jenkins SF, Wand W, Wang Y, LaCava M,

Yudt MR, Thompson CC, Freedman LP, Chung JH and Nagpal S (2008) Liver X receptor is a therapeutic target for photoaging and chronological skin aging. *Mol Endocrinol.* **22**: 2407-2419.

Court WA, Hendel JG and Elmi J (1996) Reversed-phase high-performance liquid chromatographic determination of ginsenosides of *Panax quinquefolium*. *J Chromatogr A.* **755:** 11-17.

Cheung LW, Leung KW, Wong CK, Wong RN and Wong AS (2010) Ginsenoside-Rg1 induces angiogenesis via non-genomic crosstalk of glucocorticoid receptor and fibroblast growth factor receptor-1. *Cardiovasc Res* **89**: 479-425.

de Smet PA (2002) Herbal remedies. *N Engl J Med* **347**: 2046-2056.

Hsieh CY, Hsiao HY, Wu WY, Liu CA, Tsai YC, Chao YJ, Wang DL and Hsieh HJ (2009) Regulation of shear-induced nuclear translocation of the Nrf2 transcription factor in endothelial cells. *J Biomed Sci* **16**: 12.

Hwang YP and Jeong HG (2010) Ginsenosides Rb1 protects against

6-hydroxydopamine-induced oxidative stress by increasing heme oxygenase-1 expression through an estrogen receptor-related PI3K/Akt/Nrf2-dependent pathway in human dopaminergic cells. *Toxicol Appl Pharmacol* **242**: 18-28.

Jeong WS, Kim IW, Hu R, and Kong AN (2004) Modulatory properties of various natural chemopreventive agents on the activation of NF-kappaB signaling pathway. *Pharm Res* **21**: 661–670.

Kim KC, Kang KA, Zhang R, Piao MJ, Kim GY, Kang MY, Lee SJ, Lee NH, Surh YJ and Hyun JW (2010) Up-regulation of Nrf2-mediated heme oxygenase-1 expression by eckol, a phlorotannin compound, through activation of Erk and PI3K/Akt. *Int. J BiochemCell Biol* **42**: 297–305.

Köhle C and Bock KW (2007) Coordinate regulation of Phase I and II xenobiotic metabolisms by the Ah receptor and Nrf2. *Biochem Pharmacol* **73**: 1853- 1862.

Kwok HH, Ng WY, Yang MS, Nai KM, Wong RN and Yue PY (2010) The ginsenosides protopanaxatriol protects endothelial cells from hydrogen peroxide-induced cell injury and cell death by modulating intracellular redox status.

Free Radic Biol Med **48**: 437-445.

Lee YJ, Chung E, Lee KY, Lee YH, Huh B and Lee SK (1997) Ginsenoside-Rg1, one of the major active molecules from Panax ginseng, is a functional ligand of glucocortocoid receptor. *Mol Cell Endocrinol* **133**:135-140.

Li LH, Stantom JD, Tolson AH, Luo Y and Wang H (2009) Bioactive Terpenoids and Flavonoids from Ginkgo Biloba Extract Induce the Expression of Hepatic Drug-Metabolizing Enzymes Through Pregnane X Receptor, Constitutive Androstane Receptor, and Aryl hydrocarbon Receptor-Mediated Pathways. *Pharm Res* **26**: 872-882.

Liao Y and Hung MC (2010) Physiological regulation of Akt activity and stability. *Am J Transl Res* **2**: 19-42.

Lu MC, Lai TY, Hwang JM, Chen HT, Change SH, Tsai FY, Wang HL, Lin CC, Kuo WW and Huang CY (2009) Proliferation- and migration-enhancing effects of ginseng and ginsenoside Rg1 through IGF-I- and FGF-2-signaling pathways on RSC96 Schwann cells. *Cell Biochem Funct* **27**:186-192.

Manning BD and Cantley LC (2007) Akt/PKB Signaling: Navigating Downstream. *Cell* **129**: 1261-1274.

Malhi H, Guicciardi ME and Gores GJ (2010) Hepatocyte death: A clear and present danger. *Physiological Reviews*. **90**: 1165-1194.

Meyer UA (1996) Overview of enzymes of drug metabolism. *J Pharmacokinet Biopharm* **24**: 449-459.

Miller KP and Kenneth SR (2001) Impact of cellular metabolism on the biological effects of benzo(α)pyrene and related hydrocarbons. *Drug Metab Rev* **33**: 1-35.

Min JK, Kim JH, Cho YL, Maeng YS, Lee SJ, Pyun BJ, Kim YM, Park JH and Kwon YG (2006) 20(S)-Ginsenoside Rg3 prevents endothelial cell apoptosis via inhibition of a mitochondrial caspase pathway. *Biochem Biophys Res Commun* **349**: 987-994.

Moore LB, Goodwin B, Jones SA, Wisely GB, Serabjit-Singh CJ, Willson TM, Collins JL and Kliewer SA. (2000) St. John's wort induces hepatic drug metabolism

through activation of the pregnane X receptor. *Proc Natl Acad Sci* **97**: 7500-7502.

Nakata H, Kikuchi Y, Tode T, Hirata J, Kita T, Ishii K, Kudoh K, Nagata I and Shinomiya N (1998) Inhibitory effects of ginsenoside Rh2 on tumor growth in nude mice bearing human ovarian cancer cells. *Jpn J Cancer Res* **89**: 733-774.

Nakata K, Tanaka Y, Nakano T, Adachi T, Tanaka H, Kaminuma T and Ishikawa T (2006) Nuclear receptor-mediated transcriptional regulation in Phase I, II, and III xenobiotic metabolizing systems. *Drug Metab Pharmacokinet* **21**: 437-457.

Naspinski C, Gu XS, Zhou GD, Mertens-Talcott SU, Donnelly KC and Tian Y (2008) Pregnane X Receptor Protects HepG2 Cells from BaP-induced DNA damage. *Toxicol Sci* **104**: 67-73.

Park MW, Ha J and Chung SH (2008) 20(S)-ginsenosides Rg3 enhances glucose-stimulated insulin secretion and activates AMPK. *Bio Pharm Bull* **31**: 748-751.

Ross D (2004) Quinone reductases multitasking in the metabolic world. *Drug Metab Rev* **36**: 639-654.

Sengupta S, Toh SA, Sellers LA, Skepper JN, Koolwijk P, Leung HW, Yeung HW, Wong RN, Sasisekharan R and Fan TP (2004) Modulating angiogenesis: the yin and the yang in ginseng. Circulation **110**: 1219-1225.

Shimada T, Yun CH, Yamazaki H, Gautier JC, Beaune PH and Guengerich FP (1992) Characterization of human lung microsomal cytochrome P-450 1A1 and its role in the oxidation of chemical carcinogens. *Molecular Pharmacology*. **41**: 856-864.

Wang CZ, Aung HH, Ni M, Wu JA, Tong R, Wicks S, He TC and Yuan CS (2007) Red American ginseng: Ginsenoside constituents and antiproliferative activities of heat-processed *Panax quinquefolius* roots. *Planta Med* **73**: 669-674.

Wang H, Zou H, Kong L, Zhang Y, Pang H, Su C, Liu G, Hui M, Fu L. (1999) Determination of ginsenoside Rg3 in plasma by solid-phase extraction and high-performance liquid chromatography for pharmacokinetic study. *J Chromatgr B Biomed Sci Appl* **731**:403-409.

Wang L, Chen Y, Sternberg P and Cai JY (2008) Essential roles of the PI3 kinase/Akt

pathway in regulating Nrf2-dependent antioxidant functions in the PRE. *Invest Ophthalmol Vis Sci* **49**: 1671-1678.

Xu C, Li CY and Kong AT (2005) Induction of phase I, II and III drug metabolism/transport by xenobiotics. *Arch Pharm Res* **28**: 249-268.

Yeung EY, Sueyoshi T, Negishi M and Chang TK (2008) Identification of *Ginkgo biloba* as a Novel Activator of Pregnane X Receptor. *Drug Metab Dispos* **36**: 2270–2276.

Yong L and Mien-Chie H (2010) Physiological regulation of Akt activity and stability. *Am J of Transl Res* **2**: 19-42.

Yun TK, Lee YS, Lee YH, Kim SI and Yun HY (2001) Anticarcinogenic Effect of Panax ginseng C.A. Meyer and Identification of Active Compounds. *J Korean Med Sci* **16**: S6-18.

Zang QH, Wu CF, Duan L and Yang JY (2008) Protective effects of ginsenosides Rg3 against cyclophosphamide-induced DNA damage and cell apoptosis in mice. *Arch*

Toxicol **82**: 117-123.

Zhao Q, Zheng X, Jiang, Zhou H, Hu P (2010) Determination of ginsenoside Rg3 in human plasma and urine by high performance liquid chromatography-tandem mass spectrometry. *J Chromatogr B Analyt Technol Biomed Life Sci* **878**: 2266-2273.

Footnotes

This work was partially supported by the Central Allocation Group Research Grant of Research Grant Council, Hong Kong SAR [Grant HKBU 1/06C].

DMD Fast Forward. Published on September 28, 2011 as DOI: 10.1124/dmd.111.039503
This article has not been copyedited and formatted. The final version may differ from this version.

Legends for figures

FIG. 1. Genotoxicity of BaP. HDFs were treated with different concentrations of BaP for 24 h. In the comet assay, 200 cells were analyzed for each treatment group. (A) Distribution of tail moment and (B) mean tail moment in HDFs exposed to different concentrations of BaP. (C) Cell viability was determined by MTT method after 24 h of treatment. Results were expressed as mean ± S.D. from at least three independent experiments. $^{*}p < 0.05$, $^{**}p < 0.01$ and $^{***}p < 0.001$.

FIG. 2. Effect of ginsenosides on BaP-treated cells. Cells were co-treated with ginsenosides (10 μM) and BaP (10 μM) for 24 h. (A) Viability of HDFs was determined by MTT method. $^{**}p < 0.01$ and $^{\dagger}p < 0.05$. (B) DNA damage in HDFs was determined by TUNEL assay after treatment for 24 h. Region M1 indicated the percentage of TUNEL positive cells. (C) Comet images (100X magnification, upper panel) and the quantitative measurement of tail moment (lower panel). $^{*}p < 0.05$ and $^{\dagger}p < 0.05$. Results were expressed as mean ± S.D. from three independent experiments.

FIG. 3. Effect of PI3K inhibitor on 20(S)-Rg3 from BaP-induced DNA damage.

HDFs were pretreated with LY294002 (10 μM) for 1 h and then followed by 20(S)-Rg3 (10 μM) and BaP (10 μM). DNA damage was determined by comet assay after 24 h. Results were expressed as the mean tail moment in HDFs. $^{***}p < 0.001$, $^{\dagger\dagger\dagger}p < 0.001$ and $^{\#\#\#}p < 0.001$. Results were expressed as mean ± S.D. from at least three independent experiments. 200 cells were analyzed for each treatment group.

FIG. 4. Activation of Akt and Erk by 20(S)-Rg3. HDFs were treated with 20(S)-Rg3 (10 μM) and BaP (10 μM) for the indicated time. Phosphorylation of Akt and Erk were measured by Western blot analysis. $^{\dagger\dagger}p < 0.01$ and $^{*}p < 0.05$. Representative image was shown in the upper pane. The band intensities were quantified using Kodak Digital Science 1D (New Haven, USA) and normalized to total-Akt and total-Erk, and then fold change of p-Akt and p-Erk are quantitated relative to the vehicle control. Results were expressed as mean ± S.D. from three independent experiments.

FIG. 5. Inhibitory effect of PI3K on 20(S)-Rg3-induced Nrf2 translocation in HDFs. Cells were pretreated with LY294002 (10 μM) for 1 h and then followed by 20(S)-Rg3 (10 μM), BaP (10 μM) and L-sulforaphane (SFN) (20 μM) treatments for 2 h. Immnofluorescent staining of HDFs. Cells were stained with Nrf2 antibody,

followed by the PE-conjugated anti-rabbit secondary antibody, and then the nuclei were counterstained with DAPI. Scale bar is 20 μm.

FIG. 6. Induction of NQO1 gene repression by 20(S)-Rg3. HDFs were treated with 20(S)-Rg3 (10 μM) and BaP (10 μM) for 24 h. Real-time PCR was carried out and the results were represented as the fold-change in mRNA levels. The values represent mean ± S.D. from three independent experiments. *$p < 0.05$.

FIG. 7. TR-FRET competitiive binding assay of PXR with Rg3 and SR-12813. SR-12813, a known PXR ligand, was used as a positive control. The curves were fitted with the Prism software based on the assumption of one-site competition. Only 20(S)-Rg3 but not 20(R)-Rg3 binds with PXR. Results were expressed as mean ± S.D. from at least three independent experiments.

FIG. 8. The protective effect of 20(S)-Rg3 is dependent on PXR. (A) Efficacy of siRNA targeting PXR. After transfection of siRNAs into HepG2 cells, cell lyates were obtained, electrophoresed and PXR was detected by their respective antibodies. The results shown are representative of at least three independent experiments. Actin was used for normalization of protein loading. (B) HepG2 cells were transfected with

DMD Fast Forward. Published on September 28, 2011 as DOI: 10.1124/dmd.111.039503
This article has not been copyedited and formatted. The final version may differ from this version.

si-PXR or control si-RNA for 24 h before the treatment with BaP (10 μM) and 20(S)-Rg3 (10 μM). After 24 hr treatment, comet assay was performed to determine the extent of DNA damage, 200 cells were analyzed for each treatment. Results were expressed as mean ±S.D. from at least three independent experiments. $^{*}p < 0.05$, $^{\dagger}p < 0.05$ and $^{\#}p < 0.05$.

FIG. 9. The cytoprotective mechanism of 20(S)-Rg3 against BaP-induced DNA damage. 20(S)-Rg3 induces Akt phosphorylation through the activation of PI3K, and subsequently activates Nrf2 to translocate from cytosol into the nucleus. Nrf2 translocation can regulate the expression of phase II enzymes, NQO1, which may enhance conjugation of BaP metabolites to facilitate the elimination process. 20(S)-Rg3 can also protect cells from BaP-induced DNA damage through activation of PXR. 20(S)-Rg3 act as a functional ligand of PXR. Activated-PXR may translocate into the nucleus and eliminate BaP metabolites by regulating various DMEs. The two arrows "- - - →" and "——→" indicate the two different possible pathways that are activated by 20(S)-Rg3.

Figure 1A

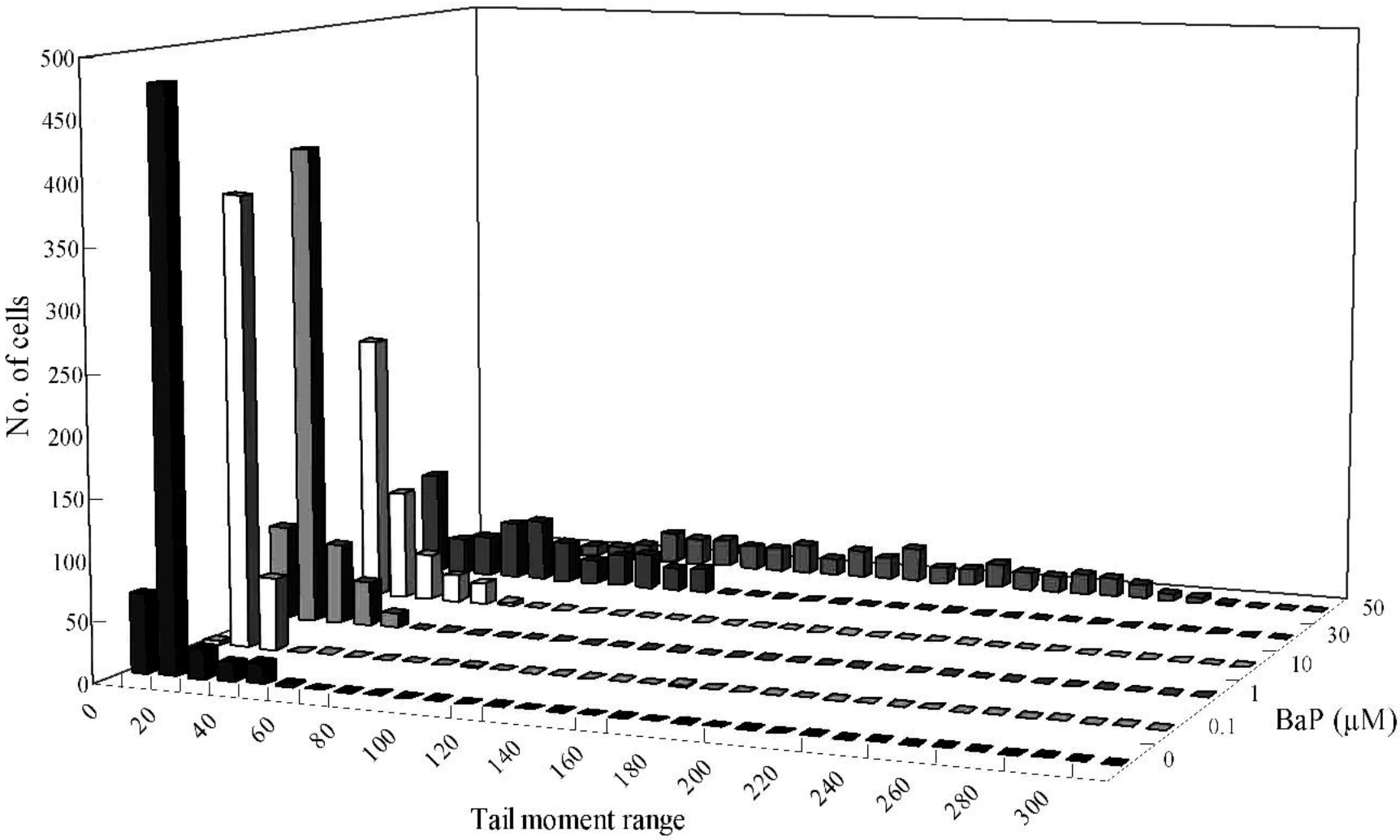
No. of cells
500
450
400
350
300
250
200
150
100
50
0
0
20
40
60
80
100
120
140
160
180
200
220
240
260
280
300
Tail moment range
50
30
10
1
0.1
0
BaP (µM)

Figure 1B

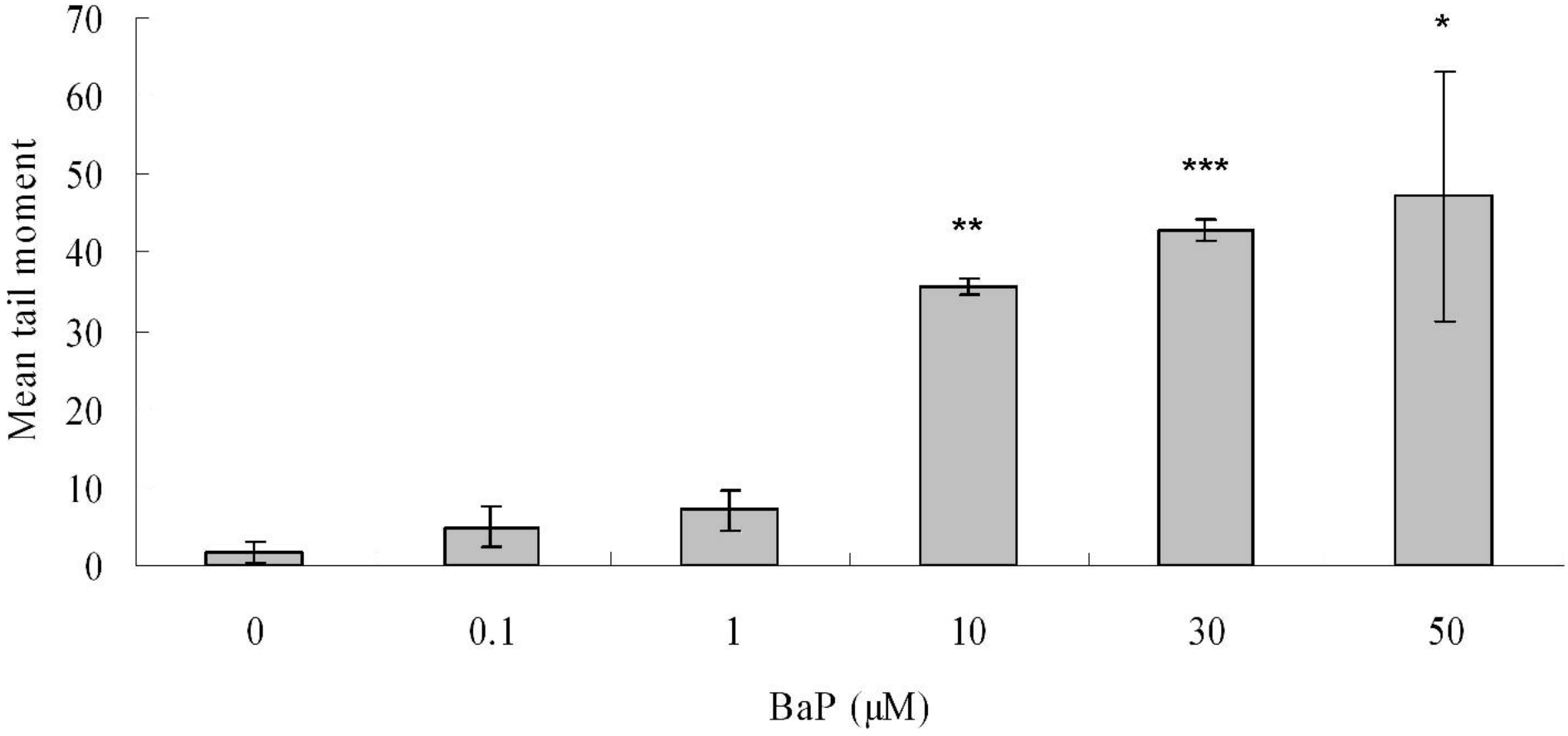

Figure 1C

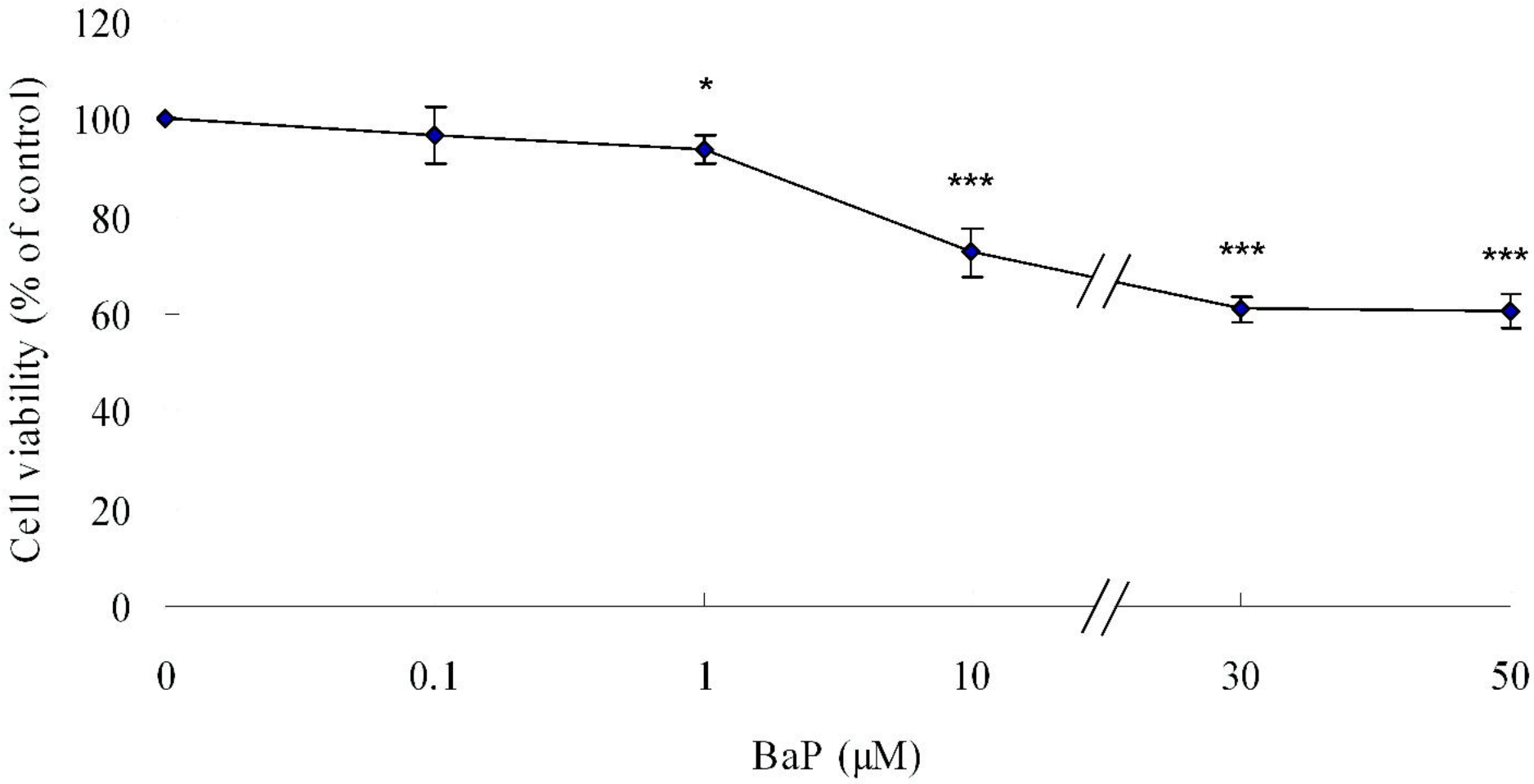
120
100
80
60
40
20
0
Cell viability (% of control)
*
***
***
***
0
0.1
1
10
30
50
BaP (μM)

Figure 2A

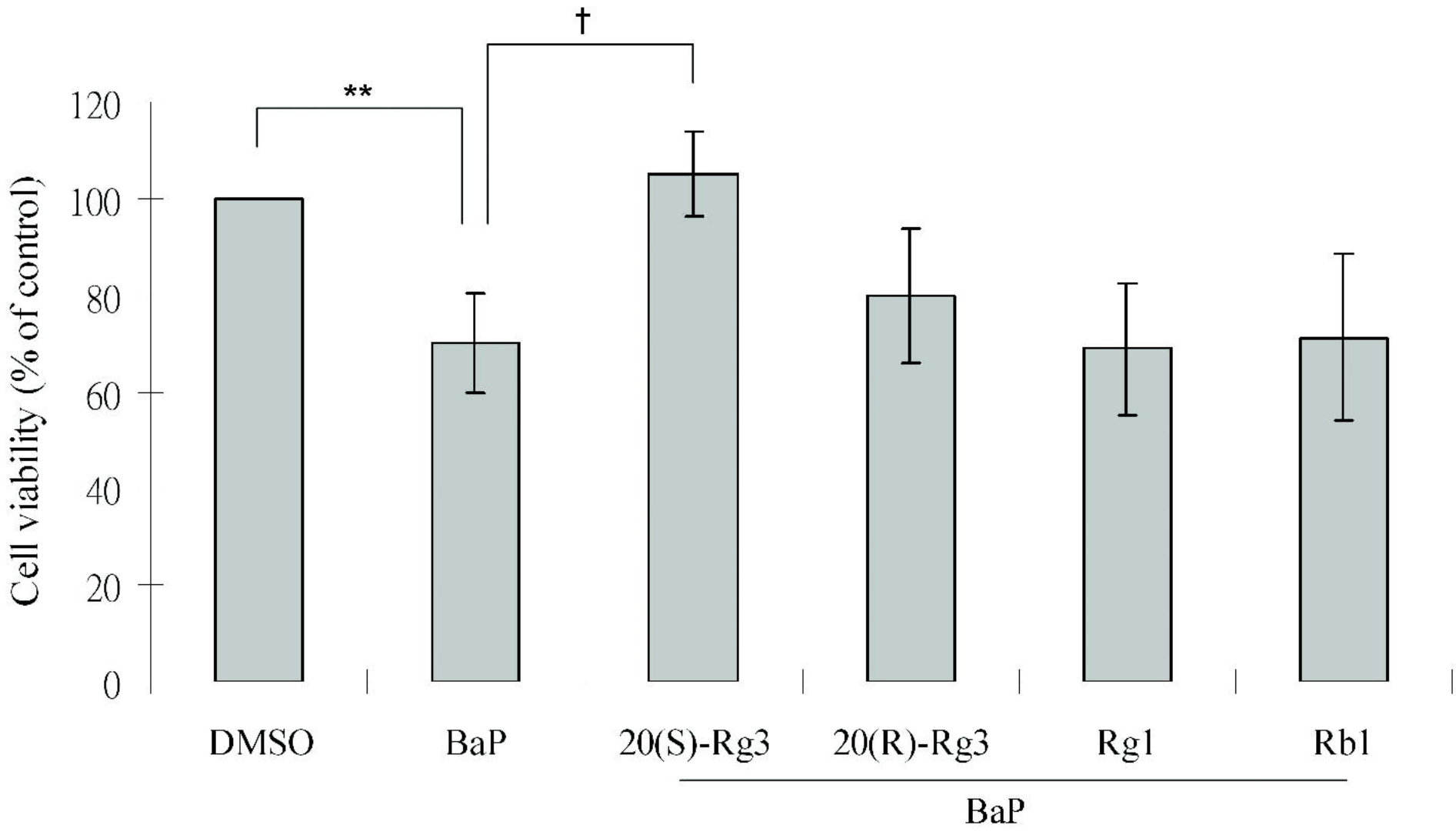
†
**
120
100
80
60
40
20
0
Cell viability (% of control)
DMSO
BaP
20(S)-Rg3
20(R)-Rg3
Rg1
Rb1
BaP

Figure 2B

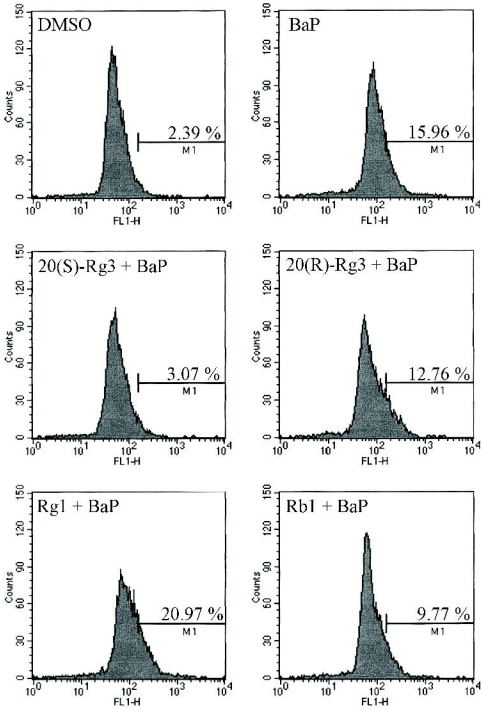
DMSO
2.39 %
M1
BaP
15.96 %
M1
20(S)-Rg3 + BaP
3.07 %
M1
20(R)-Rg3 + BaP
12.76 %
M1
Rg1 + BaP
20.97 %
M1
Rb1 + BaP
9.77 %
M1
Counts
FL1-H

Figure 2C

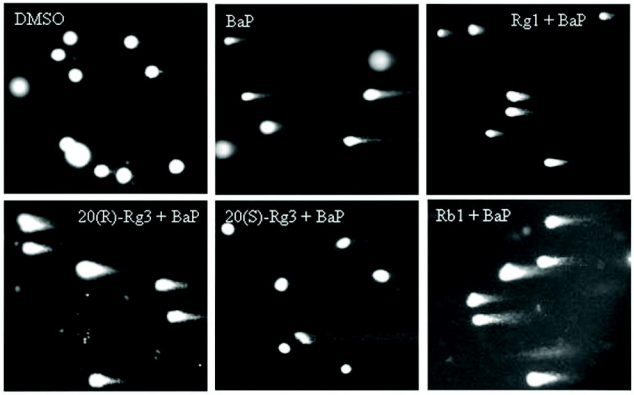
DMSO
BaP
Rg1 + BaP
20(R)-Rg3 + BaP
20(S)-Rg3 + BaP
Rb1 + BaP

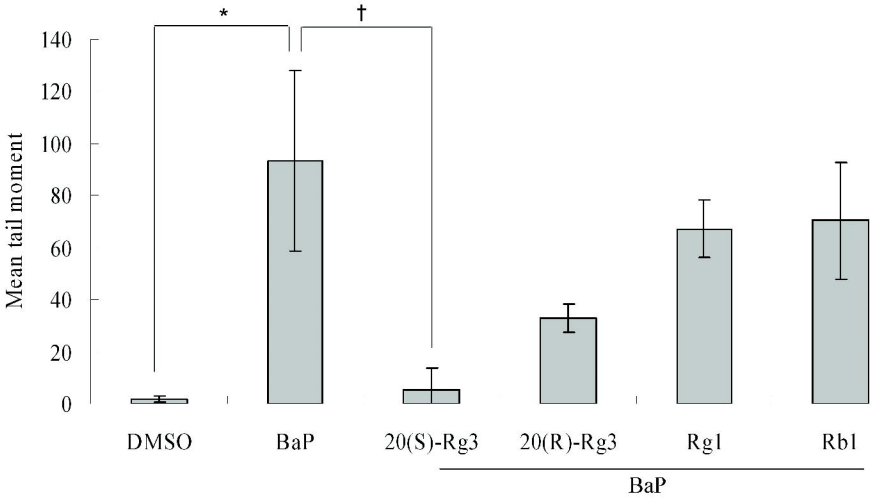
*
†
140
120
100
80
60
40
20
0
Mean tail moment
DMSO
BaP
20(S)-Rg3
20(R)-Rg3
Rg1
Rb1
BaP

Figure 3

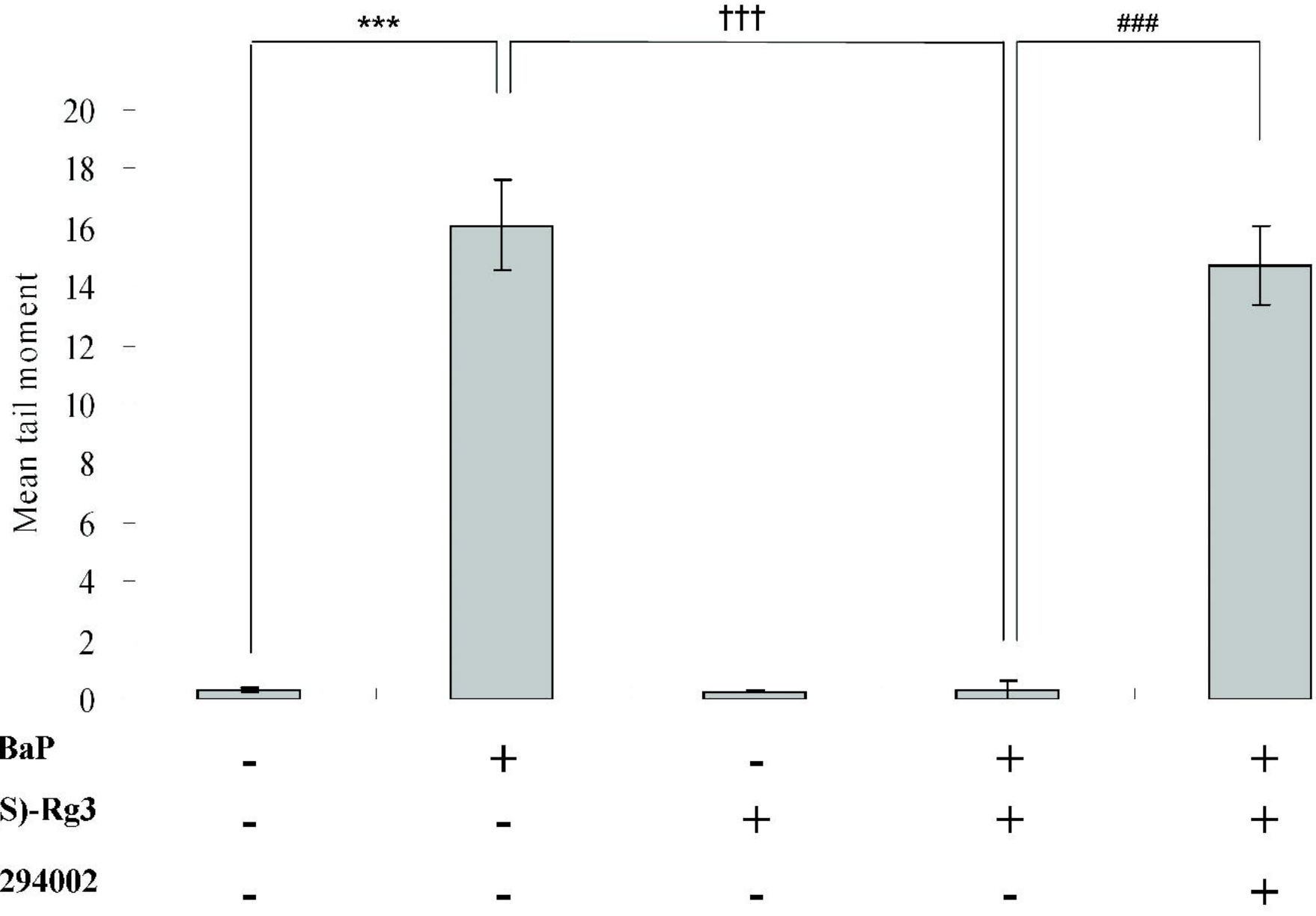

DMD Fast Forward. Published on September 28, 2011 as DOI: 10.1124/dmd.111.039503

Figure 4

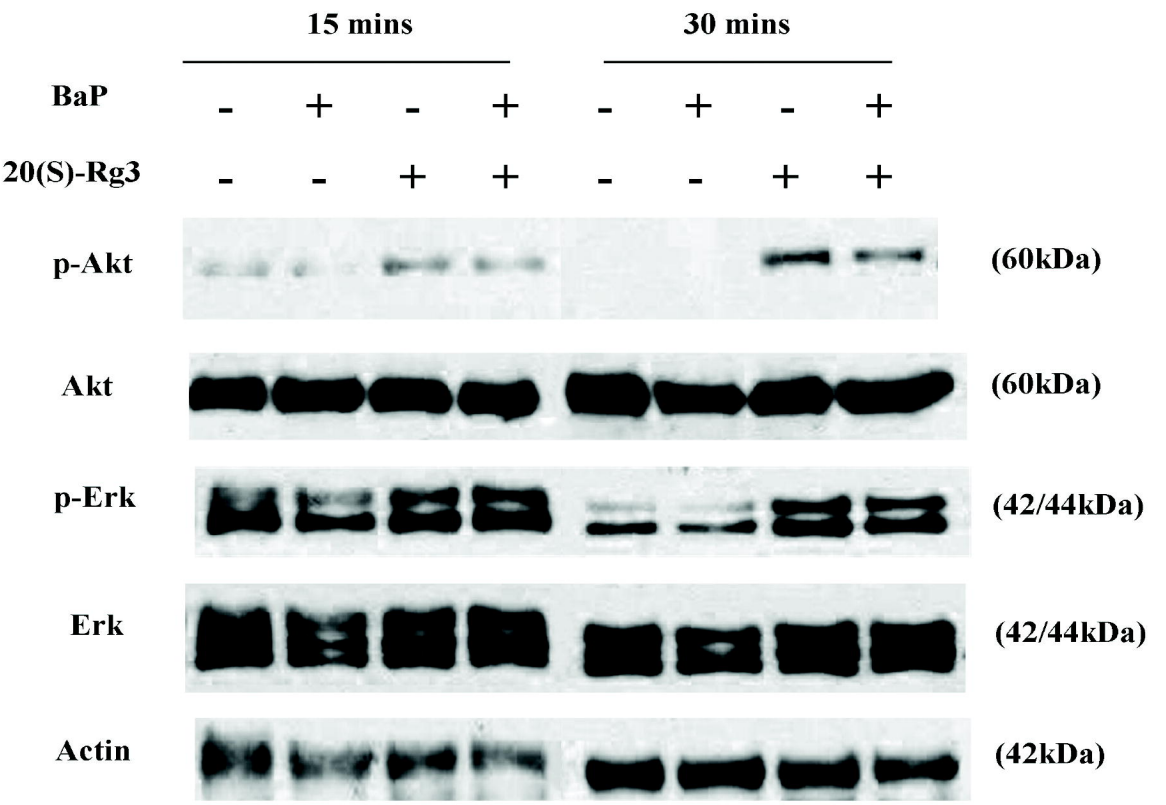

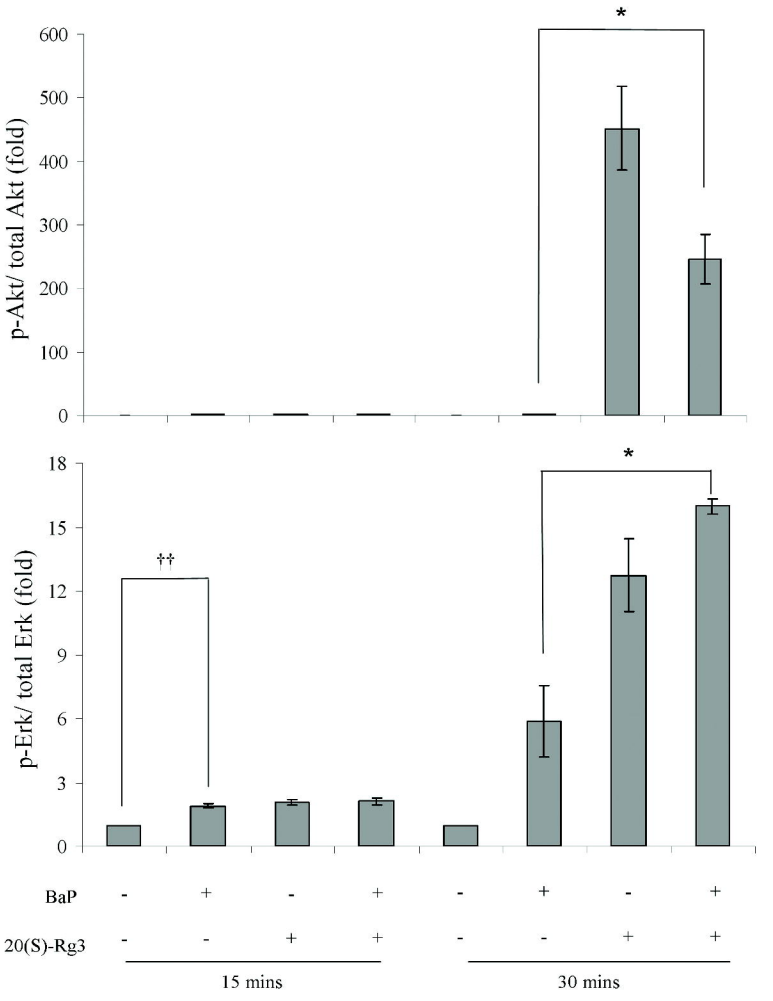

Figure 5

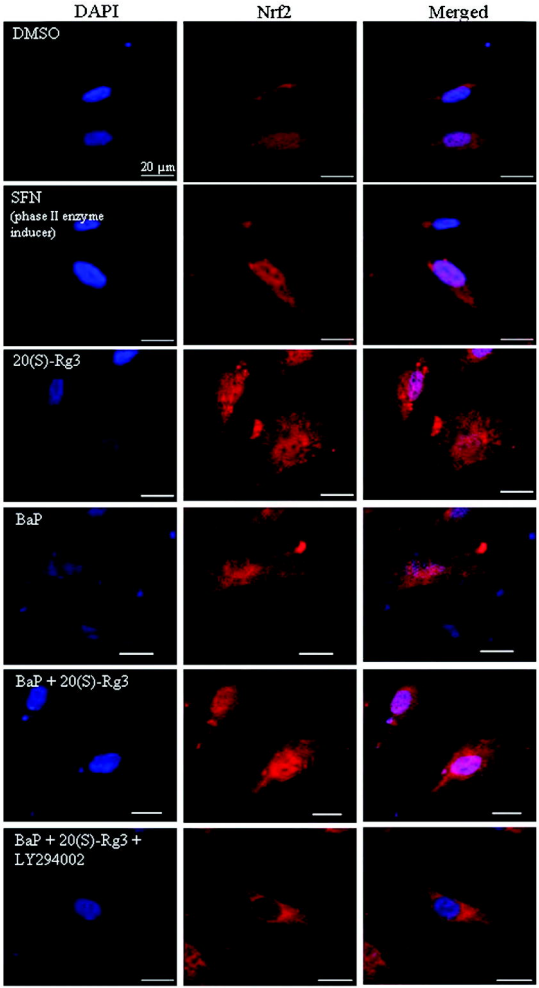
DAPI
Nrf2
Merged
DMSO
20 μm
SFN
(phase II enzyme
inducer)
20(S)-Rg3
BaP
BaP + 20(S)-Rg3
BaP + 20(S)-Rg3 +
LY294002

Figure 6

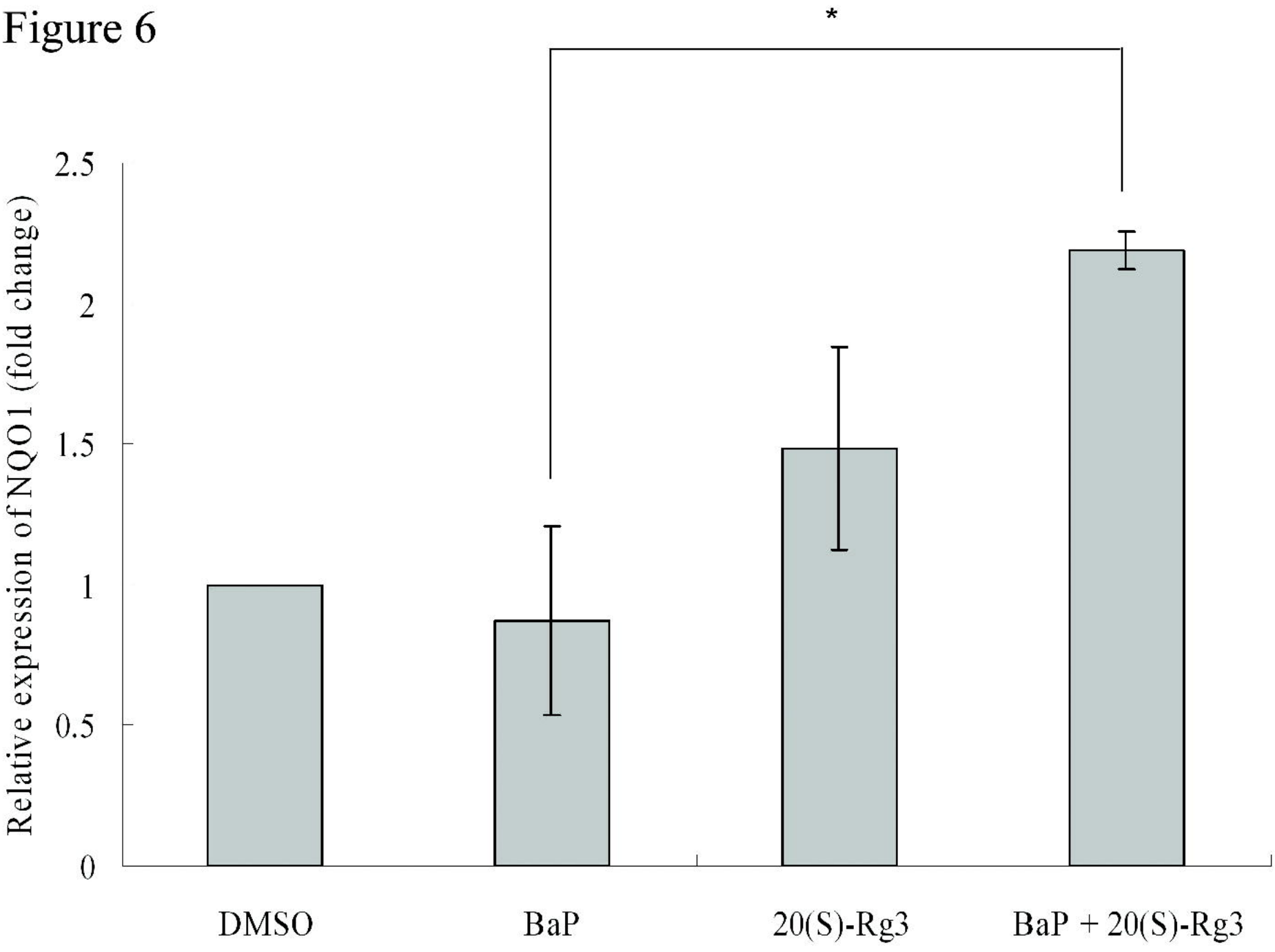
*
2.5
2
1.5
1
0.5
0
Relative expression of NQO1 (fold change)
DMSO
BaP
20(S)-Rg3
BaP + 20(S)-Rg3

Figure 7

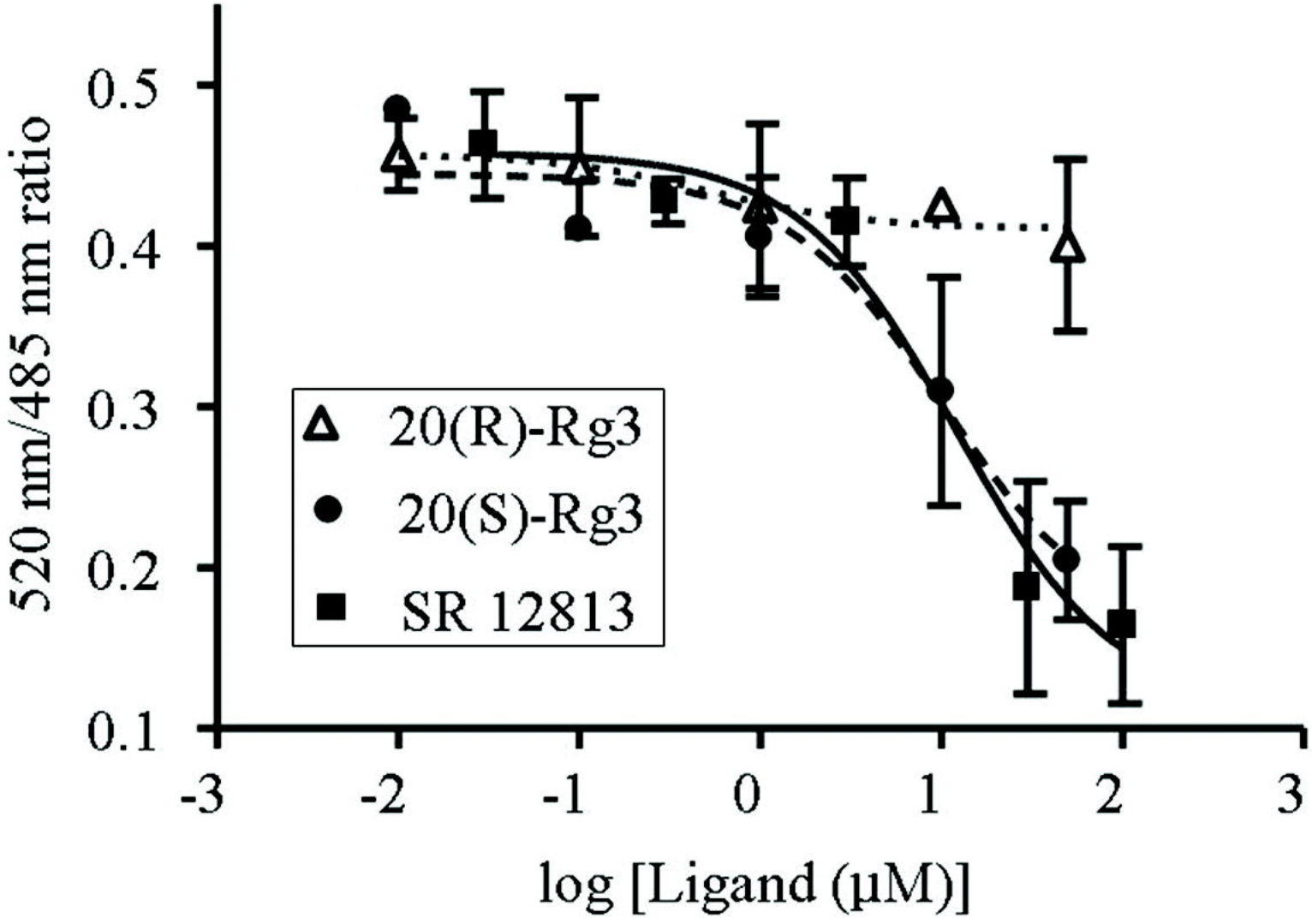
0.5
0.4
0.3
0.2
0.1
520 nm/485 nm ratio
20(R)-Rg3
20(S)-Rg3
SR 12813
-3
-2
-1
0
1
2
3
log [Ligand (μM)]

Figure 8A

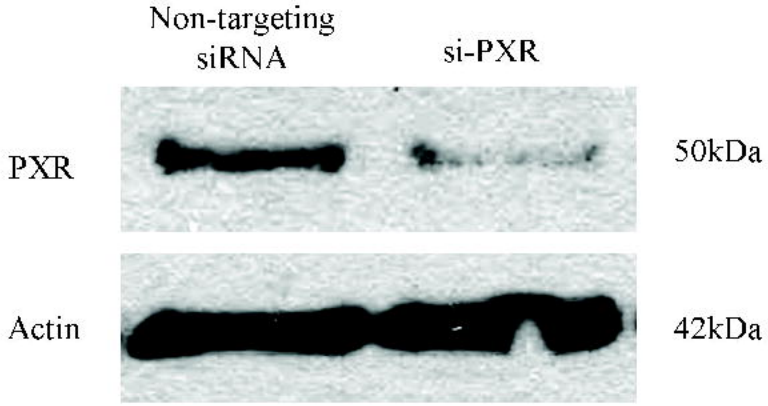

Figure 8B

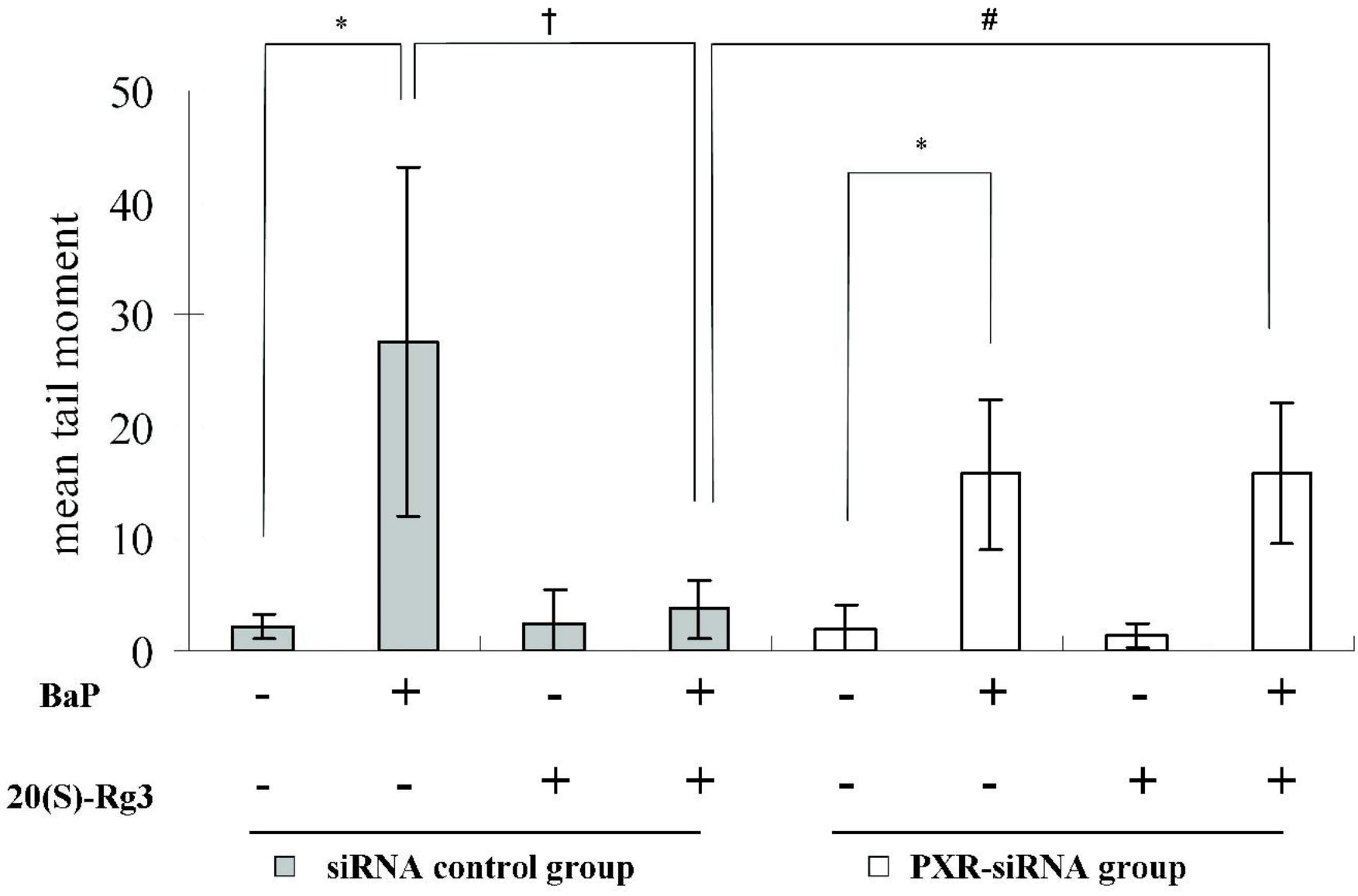
*
†
#
*
50
40
30
20
10
0
mean tail moment
BaP
- + - + - + - +
20(S)-Rg3
- - + + - - + +
siRNA control group
PXR-siRNA group

Figure 9

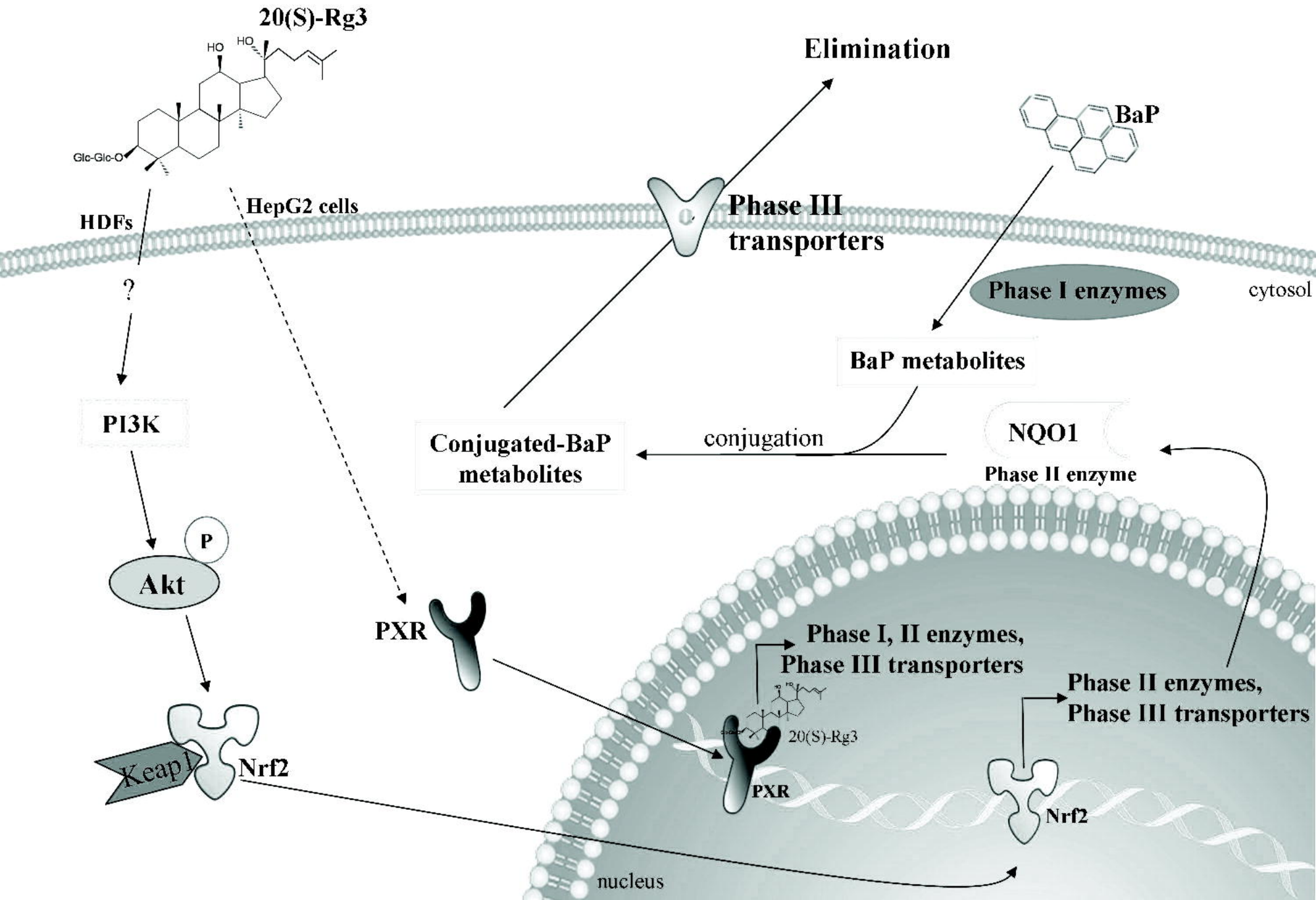
20(S)-Rg3
HO
HO
Glc-Glc-O
HDFs
HepG2 cells
?
PI3K
P
Akt
Keap1
Nrf2
PXR
Elimination
Phase III transporters
BaP
Phase I enzymes
cytosol
BaP metabolites
conjugation
Conjugated-BaP metabolites
NQO1
Phase II enzyme
Phase I, II enzymes, Phase III transporters
20(S)-Rg3
PXR
Phase II enzymes, Phase III transporters
Nrf2
nucleus